Geosynthetics, J. Kuwano & J. Koseki (eds)
© 2006 Millpress, Rotterdam, ISBN 90 5966 044 7

Soil cantilever reinforced by geosynthetics and pre-stressed steel bars

Iizuka, A.
Research Center for Urban Safety and Security, Kobe University

Hirata, M.
Toyo Construction Co. Ltd.

Ohta, H.
Dept. of International Development Engineering, Tokyo Institute of Technology

Yokota, Y.
Maeda Kosen Co. Ltd.

Keywords: geosynthetic-reinforcement, soil cantilever, compacted soil, pre-stressing, bending resistance

ABSTRACT: In this paper, the authors focus on the confining effect brought by geosynthetic-reinforcement. The reinforcement effect is not brought by the geosynthtics itself but mobilized complexly as a composite material consisting of geosynthetics and compacted soils. If the geosynthetics and the compacted soils are unified more tightly, higher reinforcement effect may be expected. Then, in this paper, presented is an experiment, that is, making soil cantilevers with compacted soils wrapped by geosynthetics which are tightly unified by prestressed steel bars. Two types of soil cantilevers were constructed. The soil structures were, first, constructed and wrapped by geosynthetics on the bases of styrene forms and, next, prestressed through the steel bars penetrated from the top surface to the bottom of the geosynthetic-reinforced soil structures. The soil cantilever was formed by melting and removing the styrene forms in order from the edge with monitoring the vertical displacements. It was found that amazing reinforcement effect appears by tightly confining the dilative deformation of compacted soils with the geosynthetics and the prestressed steel bars. The reinforcement effect is numerically investigated. A series of elasto-plastic FE numerical simulation was carried out. The compacted soil was modelled to be elasto-plastic body and the geosynthetics was expressed by the elastic material.

1 INTRODUCTION

Geosynthetic-reinforced soil structures consist of two elements: one is compacted soil and the other is geosynthetics. The strength and the rigidity of geosynthetic-reinforced soil structures do not appear as mere summation of the strength and the rigidity levels of the soil and the geosynthetic. They appear as a unified result of the mechanical interaction between the soil and the geosynthetic. The reinforcement effect is not brought by the geosynthtics itself but mobilized complexly as a composite material consisting of geosynthetics and compacted soils. If the geosynthetics and the compacted soils are unified more tightly, higher reinforcement effect may be expected. In this paper, the soil cantilevers were constructed with compacted soils and geosynthetics tightly unified by pre-stressed steel bars. The geosynthetic-reinforced soil structures were, first, constructed on the bases of styrene forms and, next, were prestressed through the steel bars penetrated from the top surface to the bottom. The experiment was performed by melting and removing the styrene forms in order from the edge and the vertical displacements at specified points on the soil structure were monitored. After that, the observed reinforcement effect was numerically investigated. A series of elasto-plastic FE numerical simulation was carried out. The compacted soil was modelled to be the elasto-plastic body and the geosynthetics was expressed by the elastic material. Through comparison with monitored results, the resistance rigidity against bending moment which was observed in the soil cantilever reinforced by combination of geosynthetics and pre-stressed steel bars was examined.

2 SOIL CANTILEVER

2.1 *Experiment procedure*

The geosynthetic-reinforced soil structures were constructed on the bases of styrene forms and cantilever shape was realized by melting and removing the styrene forms in order from the edge. Two type of soil cantilevers were considered, type A and type B (Ohta et al., 2002, Iizuka et al., 2004).

The soil cantilever, type A, was 0.7 m high, 5.7 m wide and 2.0 m deep and its feature is shown in Fig. 1. Four styrene forms (each styrene form was 0.5 m

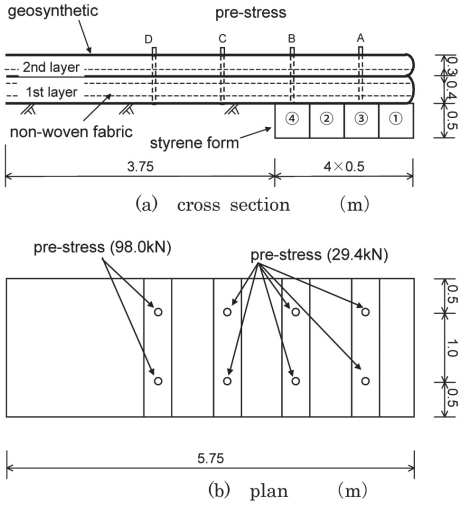

Figure 1. Soil cantilever, type A.

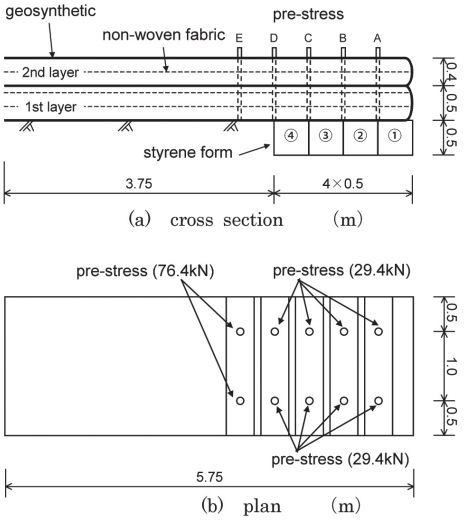

Figure 2. Soil cantilever, type B.

wide and 0.5 m high) were removed by melting them in order indicated in Fig. 1(a) to realize the soil cantilever of which span reaches 2.0 m. Geosynthetics were placed at the positions of 0.0 m, 0.4 m and 0.7 m high of the soil structure. Also, the edge of the soil structure was wrapped by nonwoven textile in order to prevent soil from flowing out. On the other hand, the soil cantilever, type B, was 0.9 m high, 5.7 m wide and 2.0 m deep as shown in Fig. 2. In the same manner, the styrene forms were removed by melting them in order from the edge as shown in Fig. 2(a) and then the soil cantilever was realized.

Geosynthetics used in the experiment was the vinyl chloride resin coated woven textile of grid shape made of aramid and polyethytene woven fabrics. The soil used in the experiment was Omma sand, of which properties are summarized in Table 1.

Table 1. Properties of Omma sand.

specific gravity of soil particle		ρ_s (t/m^3)	2.74
grain size distribution			
gravel fraction	2 mm~75 mm	(%)	2
sand fraction	75 μm~2 mm	(%)	80
silt fraction	5 μm~75 μm	(%)	11
clay fraction	less than 5 μm	(%)	7
uniformity coefficient		U_c	21.8
coefficient of curvature		U_c'	5.82
maximum grain size		(mm)	9.5

The soil was spread out in 0.1 m thick and was compacted by the vibration roller so as to achieve more than 90% of the maximum dry density. The compaction curve of Omma sand, obtained from the laboratory test, was shown in Fig. 3. Table 2 shows the initial conditions of soil structures.

The pre-stress, confining geosynthetic-reinforced soil structure, was introduced as follows. After completion of geosynthetic-reinforced soil structures, steel bars (M20), which were installed beforehand in the soil structures at intervals of 1.0 m, were tightened by the hydraulic jack up to the prescribed pre-stress value indicated in Fig. 1(b) for type A and Fig. 2(b) for type B of geosynthetic-reinforced soil structures. Herein, in order to reduce the friction force between the soil and the steel bar, the steel bars were covered with vinyl chloride tubes as shown in Fig. 4.

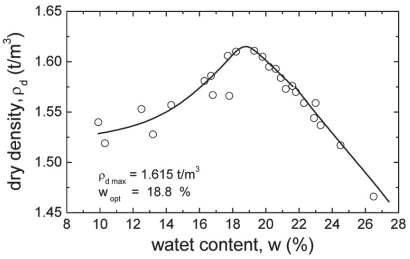

Figure 3. Compaction curve of Omma sand.

Table 2. Initial condition of two soil cantilevers

	layer	water content w (%)	drydensity ρ_d (t/m^3)
embankment A	1 st	14.89	1.385
	2 nd	14.96	1.340
embankment B	1 st	13.96	1.300
	2 nd	15.09	1.345

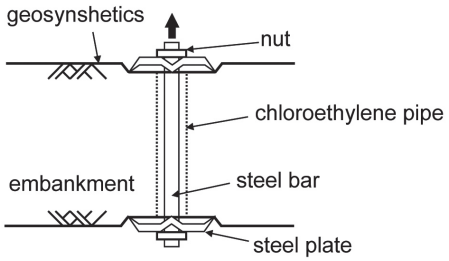

Figure 4. Introduction of pre-stress.

2.2 *Experiment result*

The soil cantilevers were realized by melting the styrene forms in order indicated in Fig. 1(a) for type A and Fig. 2(a) for type B. The vertical displacements were monitored at specified points, A to E on the geosynthetic-reinforced and pre-stressed soil structures indicated in Fig. 1 (a) for type A and Fig. 2 (a) for type B. Monitored displacements are summarized in Table 3 for type A and Table 4 for type B. In case of the soil cantilever of type A, the displacement suddenly increased when the span length reached 1.5 m by melting (removing) the styrene bases and then the soil cantilever collapsed. Photo 1 shows the overview of the soil cantilever of type A when its span length reached 1.5 m. It is found that the shear failure occurred at the root of soil cantilever. The overview of the soil cantilever of type B is shown in Photo 2, when the span length reached 1.5 m. The soil cantilever of type B, which was more highly pre-stressed than type A, did not collapse even when its span reached 2.0 m. However, the nose of the soil cantilever fell down and lay on the ground surface.

Photo 1. Overview of soil cantilever of type A when its span length reached 1.5 m.

Photo 2. Overview of soil cantilever of type B when its span length reached 1.5 m.

3 F.E. SIMULATION

3.1 *Modeling of pre-stressing process*

In the finite element simulation, first of all, the way of modelling pre-stressing process was examined.

Table 3. Monitored vertical displacement at A to C of soil cantilever of type A, see Fig. 1 (a) with widening its span.

	span length	vertical displacement (mm)		
		point A	point B	point C
initial condition	0.0 m	0	0	0
remove half of styrene form ①	–	0	0	0
remove styrene form ①	0.5 m	6	0	0
remove styrene form ②	–	21	4	0
remove half of styrene form ③	–	74	14	0
remove styrene form ③	1.5 m	412	70	1

Table 4. Monitored vertical displacement at A to E of soil cantilever of type B, see Fig. 2 (a) with widening its span.

	span length	vertical displacement (mm)				
		point A	point B	point C	point D	point E
initial condition	0.0 m	0	0	0	0	0
remove styrene form ①	0.5 m	4	3	0	0	0
remove styrene form ②	1.0 m	20	10	4	3	0
remove styrene form ③	1.5 m	145	95	39	16	0
remove half of styrene form √	-	523	371	214	96	7

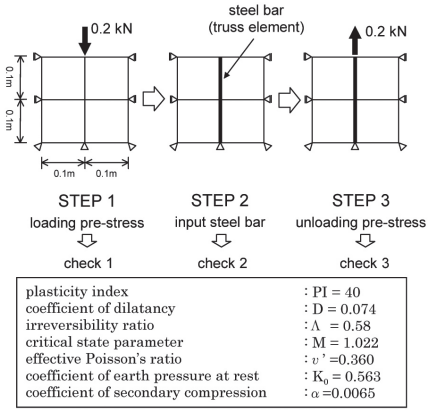

plasticity index	: PI = 40
coefficient of dilatancy	: D = 0.074
irreversibility ratio	: Λ = 0.58
critical state parameter	: M = 1.022
effective Poisson's ratio	: υ ' =0.360
coefficient of earth pressure at rest	: K_0 = 0.563
coefficient of secondary compression	: α =0.0065

Figure 5. Modelling of pre-stress.

The steel bars to which the pre-stress force was applied were modelled by elastic bar elements and 3 cases, Check 1 to 3, were considered as shown in Fig. 5. Check 1 is the case that only pre-stress was applied to the soil body (STEP 1). In Check 2, a steel bar (elastic bar element) was installed after applying the pre-stress (STEP 1 and STEP 2). And Check 3 is the case that the bar element was pulled up as shown in Fig. 5 after installation of bar elements (STEP 1, STEP 2 and STEP 3). The soil body was assumed to be an elasto-viscoplastic material and the Sekiguch-Ohta's constitutive model (Sekiguchi and Ohta, 1977) was employed. The material parameters used in the calculation are tabulated in the lower portion of Fig. 5. Figure 6 shows displacement change with time. Fig. 7 shows applied pre-stress force remaining in the bar element. It is found that, in case of Check 2, no pre-stress remains in the steel bar and the steel bar is merely compressed with time. Therefore, it can be concluded that Check 3 is the most appropriate way to model the pre-stress effect.

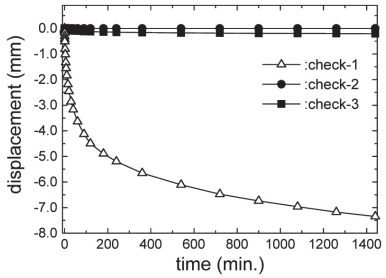

Figure 6. Displacement change with time.

3.2 *Specification of input parameters.*

A series of shear box tests for Omma sand was carried out in the laboratory to determine the soil parameters. Specimens having different water contents from 5% up to 25% to cover the natural water content in the field were prepared and used in the laboratory tests. The compressibility of Omma sand is shown in Fig. 8, which is a typical result obtained from the consolidation test in the shear box. After the specimen was consolidated with the prescribed vertical stress, it was sheared under the condition of constant volume. Figure 9 shows the effective stress paths obtained from the shear process. Input parameters needed in the computation were estimated following a systematic procedure shown in Fig. 10.

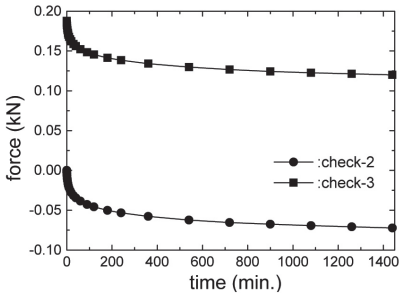

Figure 7. Calculated pre-stress working to steel bar.

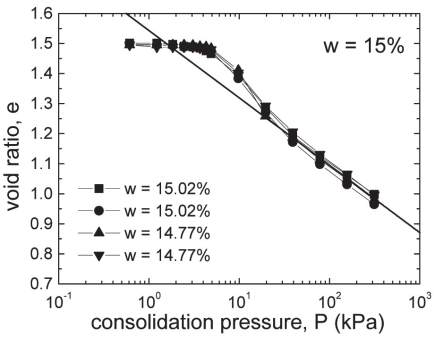

Figure 8. Compressibility of Omma sand (w = 15%).

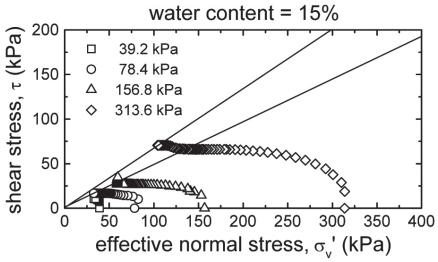

Figure 9. Effective stress paths during shearing.

Thus estimated input parameters for Omma sand are tabulated in Table 5. The compressibility of Omma sand are also summarized as a relationship between the dry density and the effective normal stress for various water contents (Fig. 11). From this figure,

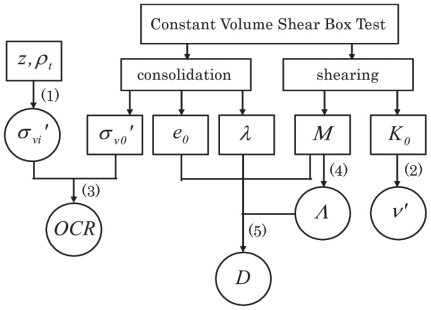

(1) $\sigma'_{vi} = \rho_t \cdot z$
(2) $\nu' K_0/(1 + K_0)$
(3) $OCR = \sigma'_{v0}/\sigma'_{vi}$
(4) $\Lambda = M/1.75$
(5) $D = \lambda\Lambda/\{M(1 + e_0)\}$

Figure 10. Input parameter specification procedure.

the pre-consolidation stress, which is equivalent to the compaction effect, can be estimated as shown in Fig. 11. Thus estimated pre-consolidation stresses for each layer of soil cantilevers are summarized in Table 6. Figure 12 shows the uniaxial extension test 100 result for the geosynthetics used in the experiment. The geosynthetics were modelled by the elastic bar

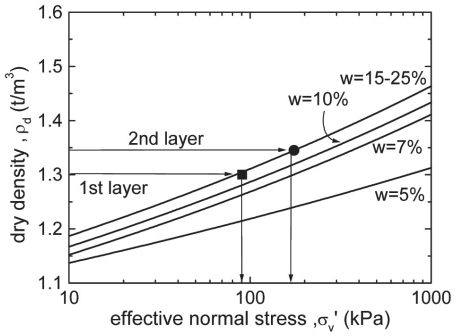

Figure 11. Dry density and consolidation stress relation.

Table 5. Estimated material parameters of Omma sand

critical state parameter, M	1.41
coefficient of earth pressure at rest, K_0	0.49
irreversibility ratio, Λ	0.80
effective Poisson's ratio, ν′	0.33

Table 6. Estimated pre-consolidation stress equivalent to compaction effect.

	1st layer	2nd layer
effective overburden pressure σ'_{vi} (kPa)	9.71	2.99
pre-consolidation pressure σ'_{v0} (kPa)	87.61	180.71
initial void ratio, e_0	1.11	1.04
over-consolidation ratio OCR	9.02	60.44

element in the simulation and its input parameters can be estimated from Fig. 12 as tabulated in Table 7. Also, the elastic constants of steel bars are shown in Table 8.

3.3 *Simulation results of soil cantilever*

Geosynthetic-reinforced and pre-stressed soil cantilevers were numerically simulated. In this paper, simulation results for the soil cantilever of type B, see Fig. 2, is presented and discussed. The finite element model is shown in Fig. 13. The prestressing process was modelled based on the preliminary study

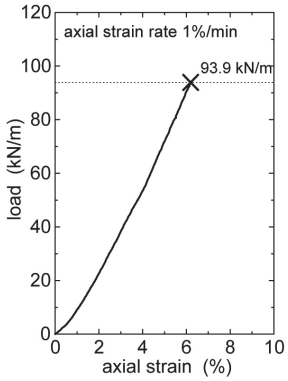

Figure 12. Uniaxial extension result of geosynthetics.

Table 7. Elastic constants for geosynthetics.

cross-sectional area A (m^2)	Young's modulus E (kN/m^2)
3.2×10^{-4}	4860800

Table 8. Elastic constants for steel bar.

cross-sectional area A (m^2)	Young's modulus E (kN/m^2)
3.14×10^{-4}	2.06×10^8

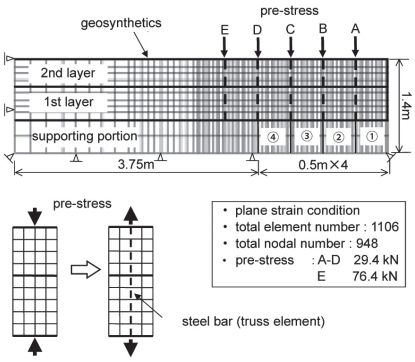

Figure 13. F.E. model of soil cantilever, type B.

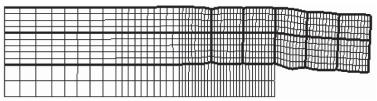

Figure 14. Deformed mesh when the span is 1.5 m.

Figure 15. Shear strain distribution when the span is 1.5 m.

Figure 16. Volumetric strain distribution when the span is 1.5 m.

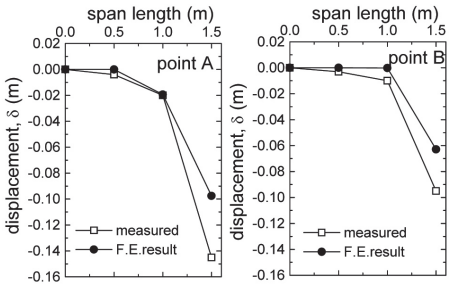

Figure 17. Vertical displacements st points, A and B.

described in 3.1 of this paper. The styrene forms were modelled to be very stiff elastic bodies and the simulation began with removing them. Figure 14 shows the computed deformation when the span length reached 1.5 m. Figures 15 and 16 indicate the shear strain and the volumetric strain distributions, respectively. Herein note that the compression is positive for the volumetric strain. It is found that the shear strain concentrates at the root of soil cantilever structure and also the dominant dilation is localized at the same portion. This means that the reinforcement effect is brought by preventing the compacted soil from dilating under shearing because the compacted soil is tightly confined by pre-stress and geosynthetics. Figure 17 indicates comparison between the computed and the measured vertical displacements at the points of A and B (see, Fig. 13). The difference of them increases with extension of the span length and the computed displacement is smaller than the measured one. Figure 18 indicates the change of remaining pre-stress, which was monitored at another field test (Ohta et al., 2002, Iizuka et al., 2004). The and gets settled into about 42% of initially applied pre-stress.

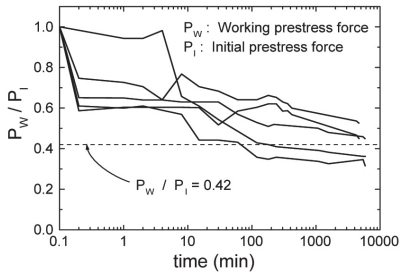

Figure 18. Decrease of remaining pre-stress with time.

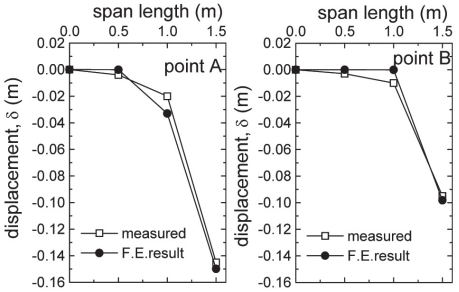

Figure 19. Computed vertical displacements considering decrease of pre-stress with time.

Then, when the decrease of pre-stress is taken into account in the numerical simulation, the computed displacements at the points of A and B are plotted as in Fig. 19 and happen to well agree with the monitored displacements.

4 CONCLUDING REMARKS

Pre-stressed geosynthetic-reinforcement effect was discussed throughout not only the field experiment for the 'soil cantilever' but also the non-elastic numerical simulation for it considering the dilatancy characteristics of compacted soil. It is found that the reinforcement effect dominantly appears when the dilative deformation is tightly confined by geosynthetics.

REFERENCES

Iizuka, A., Hirata, M., Ohta, H., Kawai, K. and Yokota, Y. (2004), The role of numerical simulation for geosynthetic reinforced soil structures – from laboratory tests to full scale structures –, *Geo Asia 2004, Invited Lecture at ISSMGE TC9 Sponsored Session, Proceedings of the 3rd Asian regional Conference on Geosynthetics,* Seoul, Korea, pp. 153-172.

Ohta, H., Maeda, Y., Nishimoto, T., Ohmori, K., Yamakami, T., Iizuka, A. and Kobayashi, I. (2002), A series of trial embankments of reinforced earth, *Proc of 7th International Conference on Geosynthetics,* IGS, pp. 307-312.

Sekiguchi, H. and Ohta, H. (1977), Induced anisotropy and time dependency in clays, *Proc. 9th ICSMFE, Specialty Session 9*, Tokyo, pp. 229-237.